

Fine-Tuning of the Spin-Crossover properties on Fe(III)

Complexes via Ligand design

Supporting Information

Daniel Vidal^[1,2], Jordi Cirera^[1] and Jordi Ribas-Arino^[2]**

[1] Departament de Química Inorgànica i Orgànica and Institut de Recerca de Química Teòrica i Computacional, Universitat de Barcelona, Diagonal 645, 08028 Barcelona, Spain

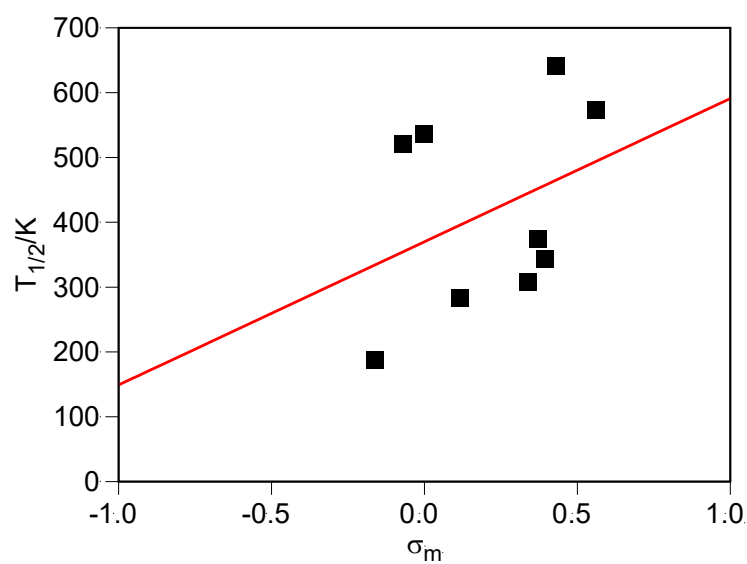
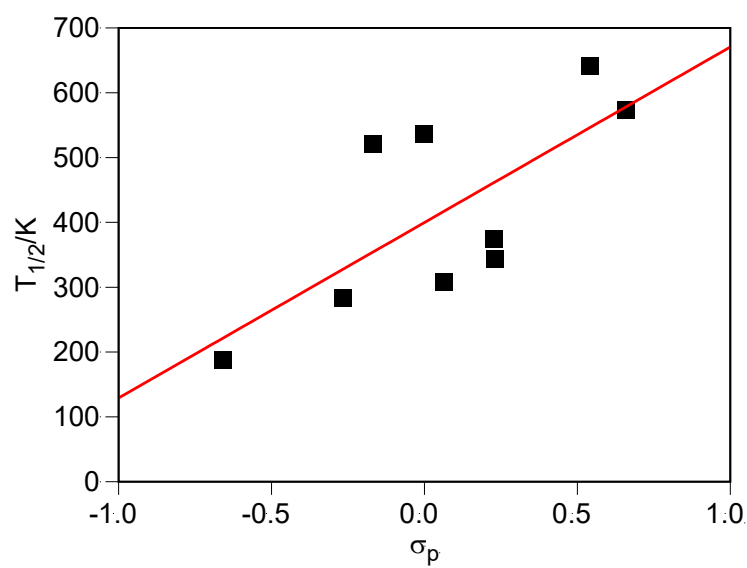
[2] Departament de Ciència de Materials i Química Física and Institut de Recerca de Química Teòrica i Computacional, Universitat de Barcelona, Diagonal 645, 08028 Barcelona, Spain

e-mail: j.ribas@ub.edu

e-mail: jordi.cirera@qi.ub.es

$T_{1/2}$ for $[\text{Fe}(\text{L}_1^{\text{R}})(\text{im})_2]^+$ vs. $\sigma_{\text{p}}/\sigma_{\text{m}}$ constant correlation	S1
$T_{1/2}$ for the $[\text{Fe}(\text{L}_2^{\text{Rp/Rm}})(\text{im})_2]^+$ vs. $\sigma_{\text{p}}/\sigma_{\text{m}}$ constant correlation	S2
NBO charges correlations for $[\text{Fe}(\text{L}_1^{\text{R}})(\text{im})_2]^+$ and $[\text{Fe}(\text{L}_2^{\text{Rp/Rm}})(\text{im})_2]^+$ systems	S3
Mulliken charges correlations for $[\text{Fe}(\text{L}_1^{\text{R}})(\text{im})_2]^+$ and $[\text{Fe}(\text{L}_2^{\text{Rp/Rm}})(\text{im})_2]^+$	S4
NBO charges correlations for (L_1^{R}) and $(\text{L}_2^{\text{Rp/Rm}})$	S5
HOMO energy vs. $T_{1/2}$ correlations	S6
$T_{1/2}$ for the $[\text{Fe}(\text{L}_1^{\text{R}})(\text{im})_2]^+$ vs. electronegativity correlation	S7
$T_{1/2}$ for the $[\text{Fe}(\text{L}_2^{\text{Rp/Rm}})(\text{im})_2]^+$ vs. electronegativity correlation	S8
Cartesian geometries for the B3LYP* optimized geometries	S9
Available experimental data	S10

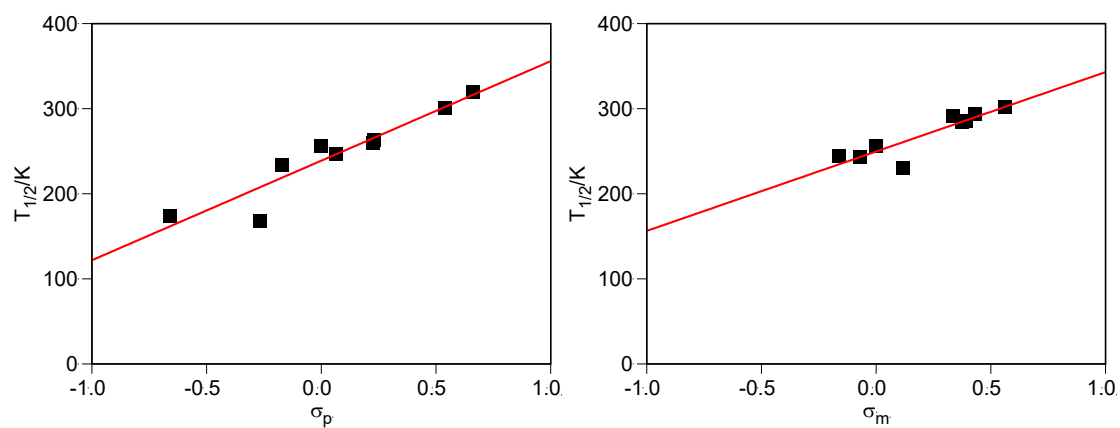
S1. $T_{1/2}$ for $[\text{Fe}(\text{L}_1^{\text{R}})(\text{im})_2]^+$ vs. $\sigma_{\text{p}}/\sigma_{\text{m}}$ constant correlation



Top, scatterplot between the computed $T_{1/2}$ and the Hammett σ_{p} constant ($R^2 = 0.51$)

Bottom, scatterplot between the computed $T_{1/2}$ and the Hammett σ_{m} constant ($R^2 = 0.13$)

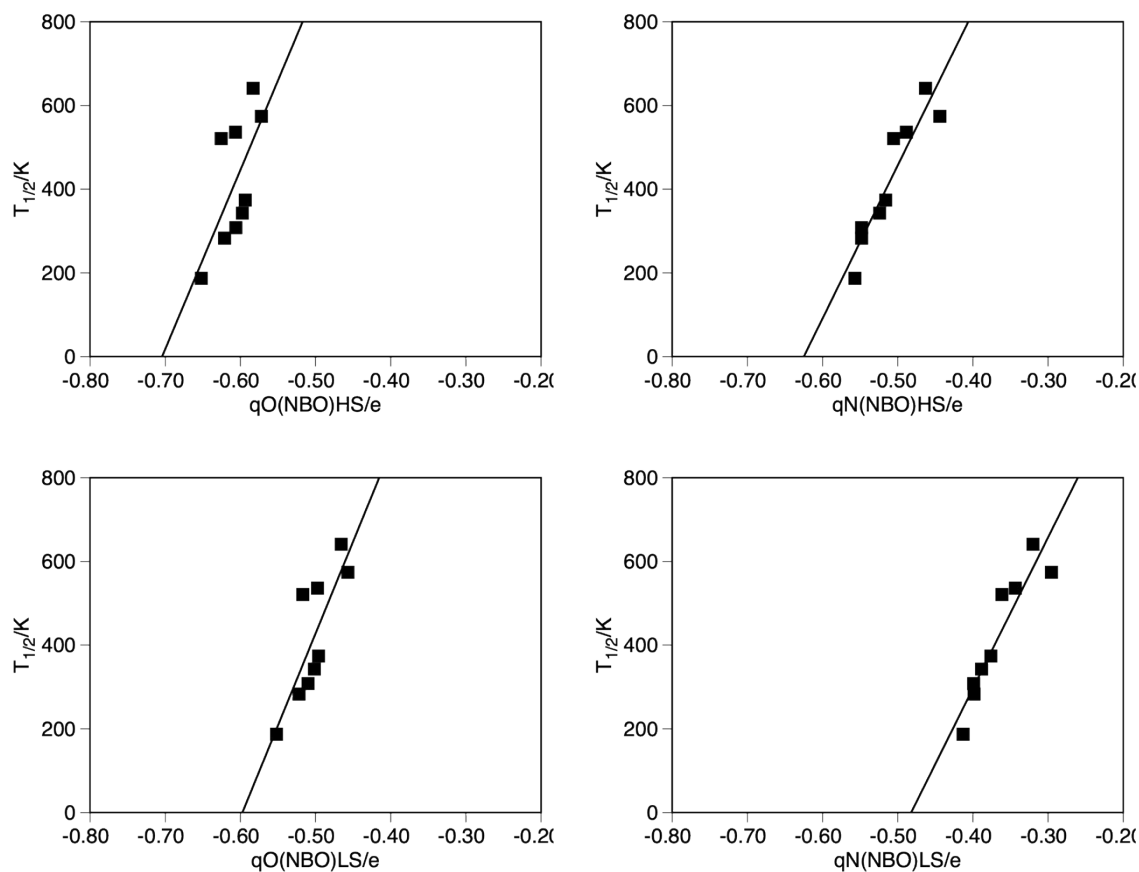
S2: $T_{1/2}$ for the $[\text{Fe}(\text{L}_2^{\text{Rp/Rm}})(\text{im})_2]^+$ vs. $\sigma_{\text{p}}/\sigma_{\text{m}}$ constant correlation



Left, correlation between the computed $T_{1/2}$ and the σ_{p} Hammett constant ($R^2 = 0.88$), and right, correlation between the computed $T_{1/2}$ and the σ_{m} Hammett constant ($R^2 = 0.79$).

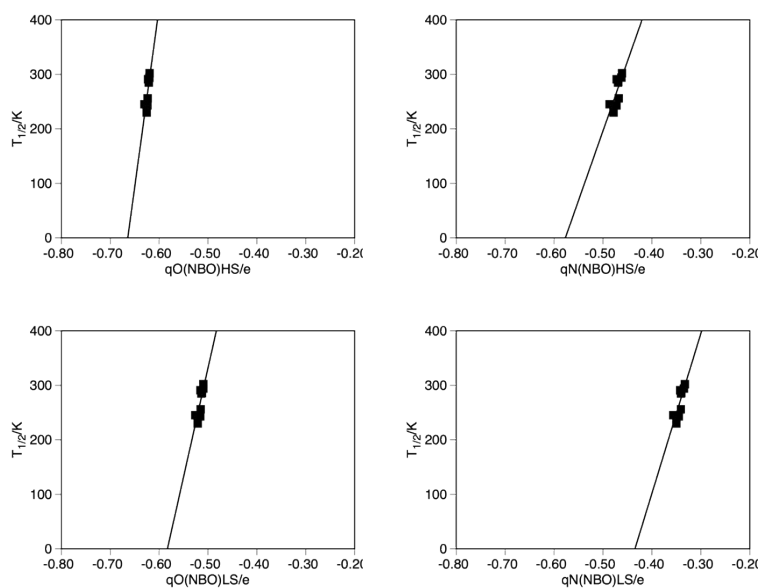
S3. NBO charges correlations for $[\text{Fe}(\text{L}_1^{\text{R}})(\text{im})_2]^+$ and $[\text{Fe}(\text{L}_2^{\text{Rp/Rm}})(\text{im})_2]^+$ systems. The following plots provide with correlations of the average NBO charge on donor oxygen atoms, $q\text{O}(\text{NBO})$, or on donor nitrogen atoms, $q\text{N}(\text{NBO})$, against $T_{1/2}$. The charges of both the high-spin (HS) and low-spin (LS) states are considered.

$[\text{Fe}(\text{L}_1^{\text{R}})(\text{im})_2]^+$ vs $T_{1/2}$



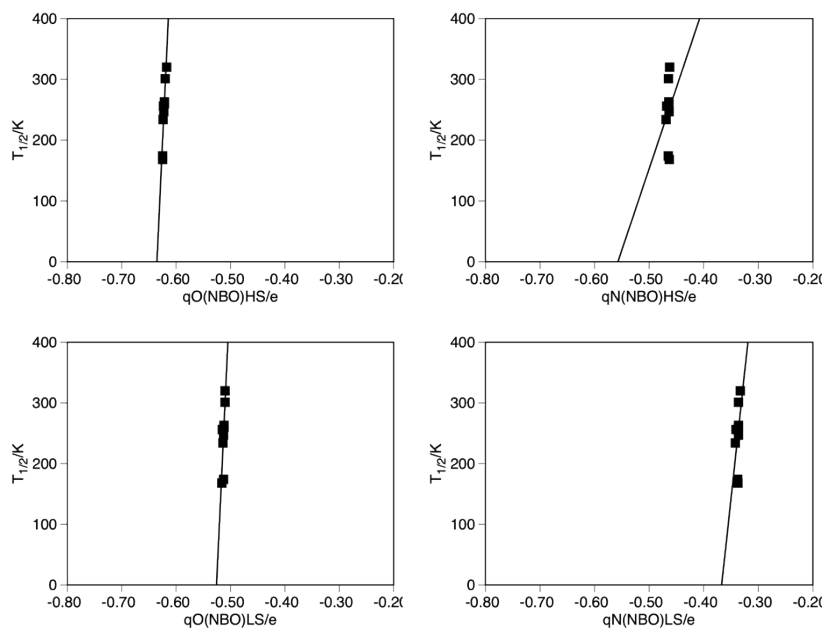
Left-Right, Top-Bottom correlation coefficients: $R^2 = 0.44$, $R^2 = 0.87$, $R^2 = 0.67$ and $R^2 = 0.86$

$[\text{Fe}(\text{L}_2^{\text{Rm}})(\text{im})_2]^+$ vs $T_{1/2}$



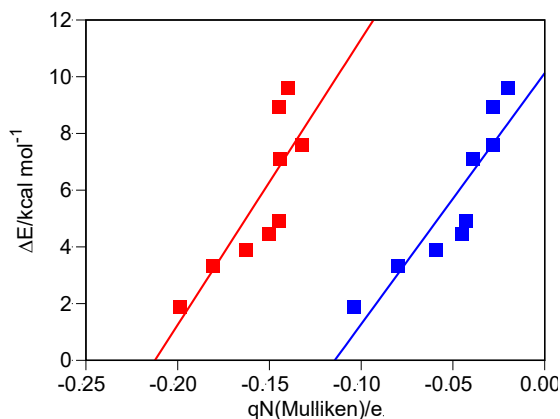
Left-Right, Top-Bottom correlation coefficients: $R^2 = 0.65$, $R^2 = 0.65$, $R^2 = 0.64$ and $R^2 = 0.66$

$[\text{Fe}(\text{L}_2^{\text{Rp}})(\text{im})_2]^+$ vs $T_{1/2}$

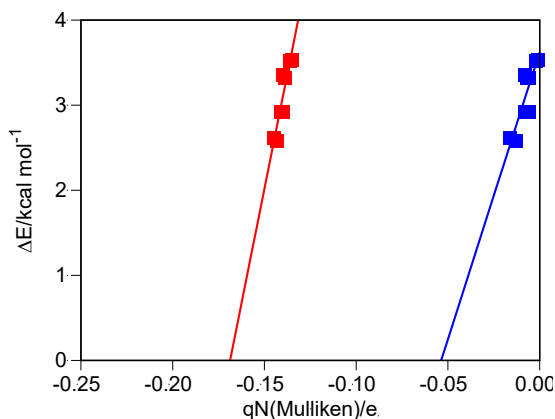


Left-Right, Top-Bottom correlation coefficients: $R^2 = 0.85$, $R^2 = 0.85$, $R^2 = 0.60$ and $R^2 = 0.19$.

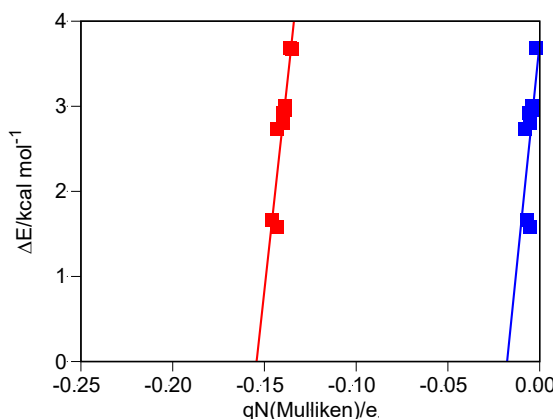
S4 Mulliken charges correlations for $[\text{Fe}(\text{L}_1^{\text{R}})(\text{im})_2]^+$ and $[\text{Fe}(\text{L}_2^{\text{Rp/Rm}})(\text{im})_2]^+$. Blue for low-spin ($S=1/2$) and red for high-spin ($S=5/2$)



Correlation between the average N Mulliken charge and the spin-state energy gap for the $[\text{Fe}(\text{L}_1^{\text{R}})(\text{im})_2]^+$ systems. ($R^2 = 0.67$ and 0.82 for high- and low-spin states respectively)

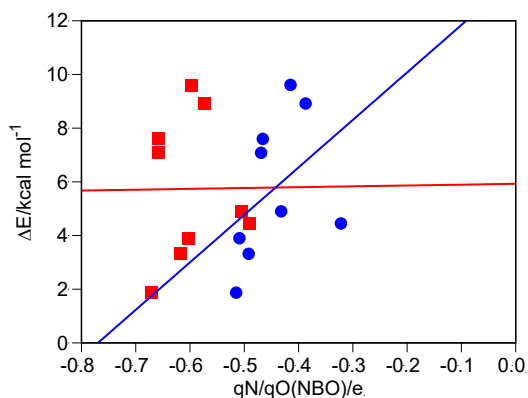


Correlation between the average N Mulliken charge and the spin-state energy gap for the $[\text{Fe}(\text{L}_2^{\text{Rm}})(\text{im})_2]^+$ systems. ($R^2 = 0.82$ and 0.76 for high- and low-spin states respectively)

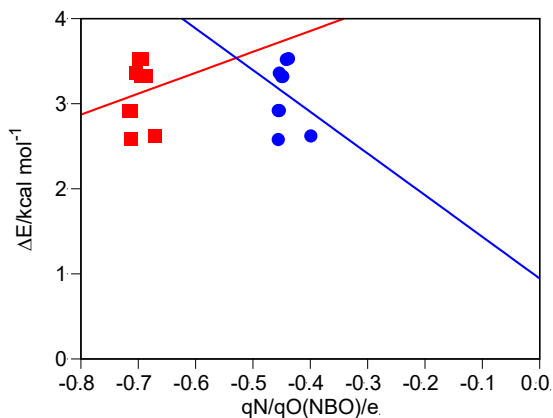


Correlation between the average N Mulliken charge and the spin-state energy gap for the $[\text{Fe}(\text{L}_2^{\text{Rp}})(\text{im})_2]^+$ systems. ($R^2 = 0.86$ and 0.48 for high- and low-spin states respectively)

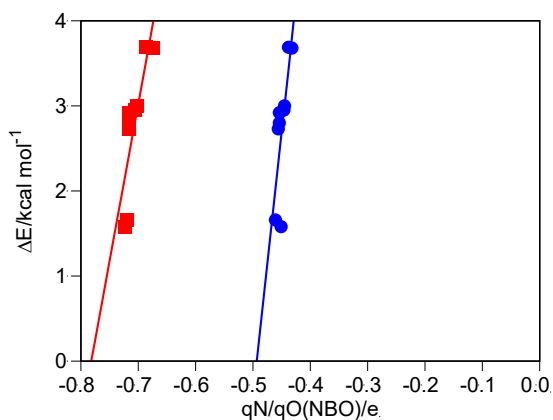
S5 NBO charges correlations for (L_1^R) and ($L_2^{Rp/Rm}$). Circle for the average NBO charge of the N-donor atoms, and squares for the average O-donor atom.



Correlation between the average N (circle) or O (squares) NBO charge of the free L_1^R ligand and the spin-state energy gap for the $[Fe(L_1^R)(im)_2]^+$ systems. ($R^2 = 0.00$ and 0.17 for oxygen and nitrogen respectively)

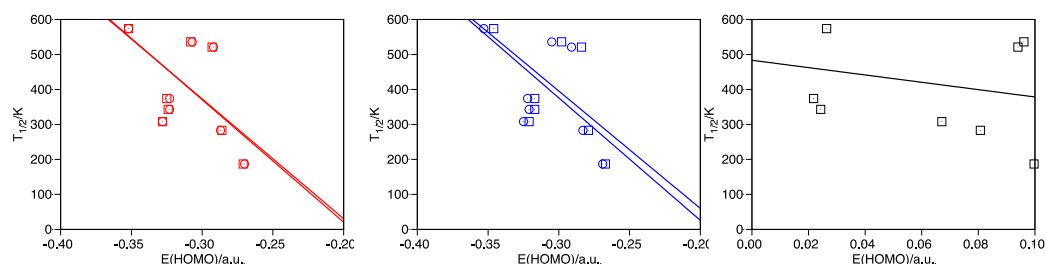


Correlation between the average N (circle) or O (squares) NBO charge of the free L_2^{Rm} ligand and the spin-state energy gap for the $[Fe(L_2^{Rm})(im)_2]^+$ systems. ($R^2 = 0.01$ and 0.05 for oxygen and nitrogen respectively)

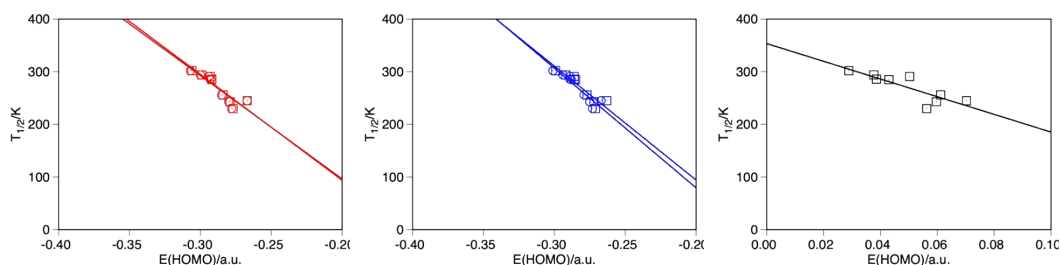


Correlation between the average N (circle) or O (squares) NBO charge of the free L_2^{Rp} ligand and the spin-state energy gap for the $[Fe(L_2^{Rp})(im)_2]^+$ systems. ($R^2 = 0.67$ and 0.58 for oxygen and nitrogen respectively)

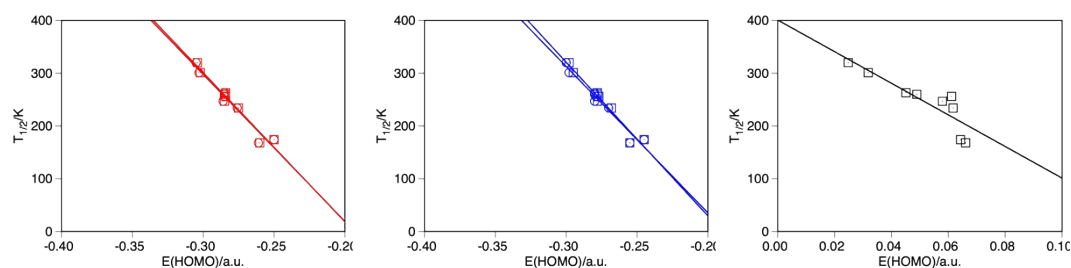
S6 HOMO energy vs. $T_{1/2}$ correlations. Red for high-spin, Blue for low-spin and black for the ligand. For the high-spin and low-spin situation, both alpha (circle) and beta (squares) HOMO energies have been used.



Energy of the HOMO vs the computed $T_{1/2}$ for the $[\text{Fe}(\text{L}_1^{\text{R}})(\text{im})_2]^+$ systems. R^2 values are 0.38 and 0.43 (high-spin alpha and beta), 0.39 and 0.45 (low-spin alpha and beta), and 0.07 (free ligand)

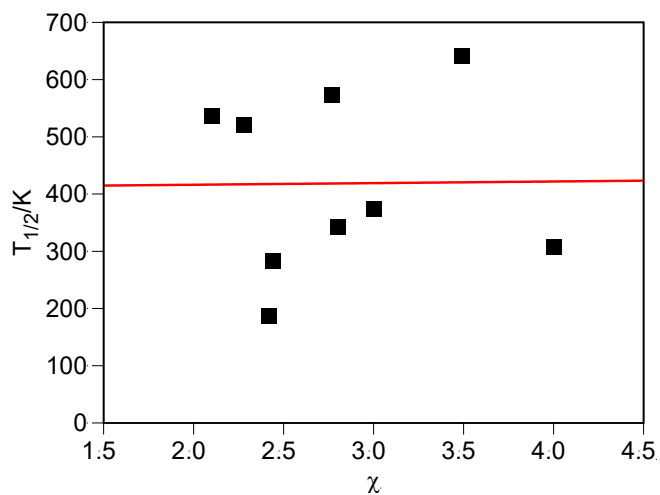


Energy of the HOMO vs the computed $T_{1/2}$ for the $[\text{Fe}(\text{L}_2^{\text{Rm}})(\text{im})_2]^+$ systems. R^2 values are 0.89 and 0.89 (high-spin alpha and beta), 0.91 and 0.92 (low-spin alpha and beta), and 0.78 (free ligand)



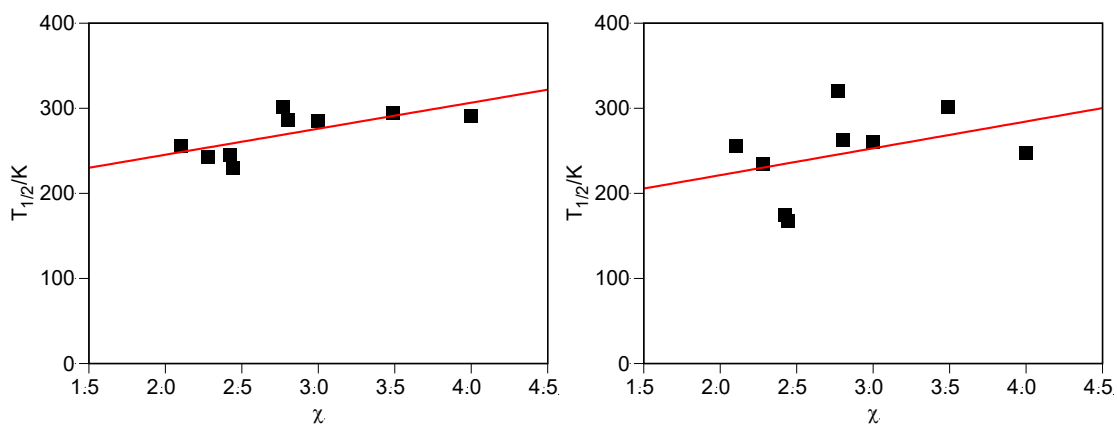
Energy of the HOMO vs the computed $T_{1/2}$ for the $[\text{Fe}(\text{L}_2^{\text{Rp}})(\text{im})_2]^+$ systems. R^2 values are 0.95 and 0.95 (high-spin alpha and beta), 0.95 and 0.95 (low-spin alpha and beta), and 0.71 (free ligand)

S7. $T_{1/2}$ for the $[\text{Fe}(\text{L}_1^{\text{R}})(\text{im})_2]^+$ vs. electronegativity correlation



Scatterplot of the substituent electronegativity¹ and the computed $T_{1/2}$ for $[\text{Fe}(\text{L}_1^{\text{R}})(\text{im})_2]^+$ ($R^2 = 0.00$)

S8. $T_{1/2}$ for the $[\text{Fe}(\text{L}_2^{\text{Rp/Rm}})(\text{im})_2]^+$ vs. electronegativity correlation



Scatterplot of the substituent electronegativity¹ and the computed $T_{1/2}$ for $[\text{Fe}(\text{L}_2^{\text{Rm}})(\text{im})_2]^+$ (left, $R^2 = 0.49$) and $[\text{Fe}(\text{L}_2^{\text{Rp}})(\text{im})_2]^+$ (right, $R^2 = 0.14$) and

S9 A data set collection of computational results is available in the ioChem-BD repository² and can be accessed via <https://doi.org/10.19061/iochem-bd-6-197>

S10 Available experimental data

Experimental data for the $[\text{Fe}(\text{L}_1^{\text{R}})(\text{im})_2]^+$ systems

<i>Substituent</i>	<i>Counterion</i>	$T_{1/2}$ (K)	<i>Reference</i>
CH ₃ ^a	[BPh ₄] ⁻	LS at all T	3

^a In addition to ESR data in powder samples, ESR measurements in DMSO frozen solutions show that the compound is LS at 298 K, which is consistent with our predicted $T_{1/2}$ value of 521 K (see Table 1 in the main text).

Experimental data for the $[\text{Fe}(\text{L}_2^{\text{Rp/Rm}})(\text{im})_2]^+$ systems

<i>Substituent</i>	<i>Counterion</i>	$T_{1/2}$ (K)	<i>Reference</i>
H	PF ₆ ⁻	78	4
H	CF ₃ SO ₃ ⁻	Gradual transition. $T_{1/2}$ not given	4
H	BPh ₄ ⁻	Gradual transition. $T_{1/2}$ not given	4
H	ClO ₄ ⁻	HS at all T	4
H	BF ₄ ⁻	HS at all T	4
H	AsF ₆ ⁻	69.4 - 74.0	5
H	SbF ₆ ⁻	105	6
OMe (<i>meta</i>) ^b	PF ₆ ⁻	~ 150	7
OMe (<i>para</i>) ^b	PF ₆ ⁻	~ 150	7
OMe (<i>meta</i>)	CF ₃ SO ₃ ⁻	192-193	8

^b Ethanolic solutions of these compounds feature thermochromism when going from liquid nitrogen temperature to room temperature, which is in line with our predicted $T_{1/2}$ values of 230 K (*meta*, Table 2 in the main text) and 168 K (*para*, Table 3 in the main text).

References:

- 1 S. G. Bratsch, *J. Chem. Educ.*, 1985, **62**, 101.
- 2 M. Álvarez-Moreno, C. de Graaf, N. López, F. Maseras, J. M. Poblet and C. Bo, *J. Chem. Inf. Model.*, 2015, **55**, 95–103.
- 3 Y. Nishida, S. Oshio and S. Kida, *Inorganica Chim. Acta*, 1977, **23**, 59–61.
- 4 M. Koike, K. Murakami, T. Fujinami, K. Nishi, N. Matsumoto and Y. Sunatsuki, *Inorganica Chim. Acta*, 2013, **399**, 185–192.
- 5 T. Fujinami, M. Koike, N. Matsumoto, Y. Sunatsuki, A. Okazawa and N. Kojima, *Inorg. Chem.*, 2014, **53**, 2254–2259.
- 6 T. Ueno, K. Miyano, D. Hamada, H. Ono, T. Fujinami, N. Matsumoto and Y.

- Sunatsuki, *Magnetochemistry*, 2015, **1**, 72–82.
- 7 T. Fujinami, M. Ikeda, M. Koike, N. Matsumoto, T. Oishi and Y. Sunatsuki, *Inorganica Chim. Acta*, 2015, **432**, 89–95.
- 8 K. Miyano, T. Nishida, H. Ono, D. Hamada, T. Fujinami, N. Matsumoto and Y. Sunatsuki, *Inorganica Chim. Acta*, 2016, **439**, 49–54.